A new approach to structural integrity assessment based on axial and radial diffusivities.

C. A. Wheeler-Kingshott[1], O. Ciccarelli[2], T. Schneider[1], D. C. Alexander[3], and M. Cercignani[4]
[1]NMR Unit, Department of Neuroinflammation, UCL Institute of Neurology, London, United Kingdom, [2]NMR Unit, Department of Brain Repair and Rehabilitation, UCL Institute of Neurology, London, United Kingdom, [3]Dept. Computer Science, UCL, Centre for Medical Image Computing, London, United Kingdom, [4]Neuroimaging Laboratory, Fondazione Santa Lucia, Rome, Italy

Introduction: Axial and radial diffusivities measured from the eigenvalues of the diffusion tensor (DT) have been shown to correlate with axonal integrity and myelin staining in animals (1-2). Since then, these quantities have been studied in several diseases, including multiple sclerosis (MS). The definition of axial diffusivity as the principal eigenvalue of the diffusion tensor relies on the assumption that the principal eigenvector is aligned with the main fiber orientation of each voxel. It has been shown (3) that in pathology this may not be the case and that a better definition of the axial and radial diffusivities relies on the characterisation of the diffusion direction based on the average DT of a healthy population of reference (4), referred to as the "super-DTI" dataset. We have defined the projected-axial and projected-radial diffusivities as the components of the individual DTs along the eigenvectors of the super-DTI dataset (4). In this work, we have compared the newly introduced projected-axial and projected-radial diffusivities with the axial and radial diffusivities calculated from the DT, showing results in patients with MS.

Methods: **(i)** Reference dataset: The super-DTI dataset was obtained from a population of 15 healthy subjects (6 males and 9 females, mean age =40±14) by following the steps described in (4). In summary, the DT of each subject was calculated using the Camino toolkit (www.camino.org) from diffusion weighted (DW) datasets acquired on a GE 1.5T scanner (60 axial-oblique slices, 61 diffusion encoding directions, b=1200 s mm^{-2}, 7 non-DW scans (b_0), voxel size 2.3×2.3×2.3mm^3, TR ≈ 20 s depending on heart rate, TE = 96 ms). Maps of FA from each subject were registered to a template FA map in MNI space (from the FMRIB software library) using fnirt, a non-linear registration tool (www.fmrib.ox.ac.uk/fsl/fnirt/index.html). The transformation matrix was then applied to the individual components of the DTs, using the PPD algorithm (5) to preserve the directional diffusion encoding information. The reoriented DT datasets were averaged and the averaged dataset was then diagonalised to obtain the eigenvalues and eigenvectors of the super-DT, which are considered the reference diffusivities ($\lambda_{1,ref}$, $\lambda_{2,ref}$, $\lambda_{3,ref}$) and their directions ($\boldsymbol{\varepsilon}_{1,ref}$, $\boldsymbol{\varepsilon}_{2,ref}$, $\boldsymbol{\varepsilon}_{3,ref}$), for a standard population of healthy subjects; **(ii)** Projected diffusivities: For each subject, j, the projected-axial, $d_{p\text{-}ax,\,j}$, and projected-radial, $d_{p\text{-}rad,\,j}$, diffusivities were defined as the projection of the DT$_j$ in standard space along $\boldsymbol{\varepsilon}_{1,ref}$ and the average of the projections along $\boldsymbol{\varepsilon}_{2,ref}$ and $\boldsymbol{\varepsilon}_{3,ref}$ respectively. We also calculated the axial and radial diffusivities, $d_{ax,\,j}$ and $d_{rad,\,j}$, as the principal eigenvalue, $\lambda_{1,\,j}$, and the average of the second, $\lambda_{2,\,j}$, and third, $\lambda_{3,\,j}$, eigenvalues of the individual DTj in standard space; **(iii)** VBM analysis: As well as for the 15 subjects that formed the super-DT dataset, we calculated $d_{p\text{-}ax,j}$ and $d_{p\text{-}rad,j}$ for two patients with MS, p_1 (female, age = 34 years, EDSS (Expanded Disability Status Scale) = 2.5, disease duration = 1.5 years) and p_2 (male, age = 55 years, EDSS = 5.5, disease duration = 7 years), and for an additional healthy control, hc, (female, age = 37 years). Using the Voxel Based Morphometry (VBM) toolkit in SPM5 (http://www.fil.ion.ucl.ac.uk/spm/software/spm5/) with a two-samples t-test, we compared the projected diffusivities for hc, p_1 and p_2 with those of the reference group. One group was set to be the 15 healthy subjects and the other group was set to be either hc, p_1 or p_2. Equal variance was assumed (6). Results are reported for $p<0.001$ uncorrected for multiple comparisons. We also compared the results of the projected diffusivities with those obtained when looking at the axial, $d_{ax,j}$, and radial, $d_{rad,j}$, diffusivities; **(iv)** White matter (WM) pathology: Pathology in MS is characterised by hyperintense signal on proton density (PD) and T_2 weighted scans. For this study, WM lesions of p_1 and p_2 were contoured on PD-weighted scans, with reference to a co-registered T_2-weighted scans from a dual spin echo acquisition (TE= 30/102ms, TR= 2500ms, voxel size = 0.94x0.7x5mm^3). The T_2 weighted scans were linearly registered to the non-diffusion-weighted b_0 scan of the super-DTI dataset, using an affine transformation from the FSL library (www.fmrib.ox.ac.uk/fsl/flirt/index.html). The transformation coefficients from T_2 to b_0-space were combined with the non-liner transformation coefficients obtained from the registration of the individual FA maps to the FA template and the resulting transformation was applied to the lesion mask file, selecting nearest neighbour interpolation.

Results: Axial diffusivity: The most remarkable result of the analysis is that in p_2 (the most disabled patient) there are areas of *decreased* projected axial diffusivity, $d_{p\text{-}ax,p2}$, compared to the controls. These areas are not always highlighted when looking at $d_{ax,p2}$ (figure 1a), indicating that the projected axial diffusivity may be more sensitive to early pathology than the axial diffusivity. In p_1 there are only a few voxels characterised by a reduced $d_{p\text{-}ax,p1}$, mostly coinciding with voxels of reduced $d_{ax,p1}$ (figure 1b). No voxels of decreased diffusivities $d_{p\text{-}ax}$ and/or d_{ax},are found in the hc. Areas of *increased* $d_{p\text{-}ax}$ are also found, especially in p2. These areas are characterised by an increase of d_{ax} too (figure 1c).

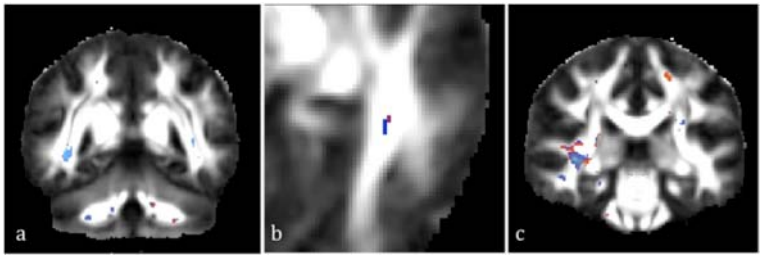

Figure 1: Results of the analysis of the projected axial, $d_{p\text{-}ax}$, and axial, d_{ax}, diffusivities. a) Areas of *decreased* $d_{p\text{-}ax,p2}$ (blue) and $d_{ax,p2}$ (red) compared to controls. b) As (a) but for p1. c) Areas of *increased* $d_{p\text{-}ax,p2}$ (blue) and $d_{ax,p2}$ (red) compared to controls. Overlapping voxels are purple.

Radial diffusivity: The analysis of the radial diffusivity showed that changes of $d_{p\text{-}rad}$ mostly coincide with similar changes of d_{rad}. In hc and p_1, areas of difference between $d_{p\text{-}rad}$ and d_{rad} compared to the corresponding measurement in the healthy population are almost identical; in p_2, areas of *increased* $d_{p\text{-}rad}$ coincide with areas of increased d_{rad}, and they seem spatially more localised (figure 2a). No areas of significant *decreased* radial diffusivities, $d_{p\text{-}rad}$ and d_{rad}, are found in any of the subjects, hc, p_1 and p_2.

WM pathology: The location of the WM lesions of p_1 and p_2 was assessed with reference to the areas of *increased* radial diffusivity and *decreased* axial diffusivity, for both the traditionally defined parameters, d_{ax} and d_{rad}, and the projected parameters, $d_{p\text{-}ax}$ and $d_{p\text{-}rad}$. Areas of *increased* axial diffusivity, for both $d_{p\text{-}ax,p2}$ and $d_{ax,p2}$, are localised within the lesion mask (not shown), while areas of *decreased* axial diffusivity are not necessarily related to the presence of focal lesions, as shown in figure 2b for the projected axial diffusivity, $d_{p\text{-}ax,p2}$. Areas of *increased* projected radial, $d_{p\text{-}rad}$, and radial, d_{rad}, diffusivities overlap marked lesions and extend beyond the boundaries as shown for p_2 in figure 2c.

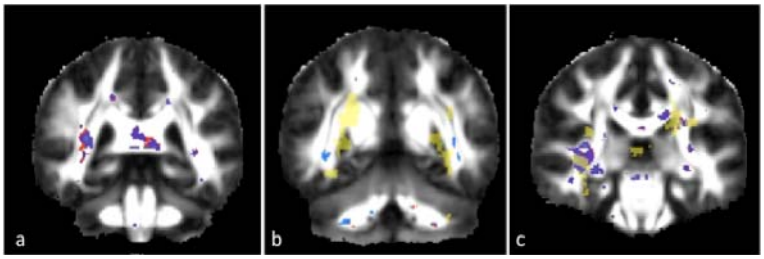

Figure 2 – a) Areas of *increased* $d_{p\text{-}rad,p2}$ (blue) and $d_{rad,p2}$ compared to controls. b) Spatial correspondence of areas of *decreased* $d_{p\text{-}ax,p2}$ (blue) and MS lesion mask (yellow). c) Spatial correspondence between areas of *increased* $d_{p\text{-}rad,p2}$ (blue) and $d_{rad,p2}$ (red) and MS lesion mask (yellow).

Conclusions: In healthy controls axial and radial diffusivities calculated from the eigenvalues of the DT are robust parameters that have been shown to be potential biomarkers for axon integrity and myelin (2). The projected axial and radial diffusivity are new parameters defined on the basis of a healthy reference super-DT dataset. Preliminary investigations show that they offer a new sensitivity to WM pathology (e.g. figure 1a) and that they have the potential to detect degeneration before the appearance of focal lesions.

References: 1. Song et al. Neuroimage. 20,1714 (2003); 2. Budde et al. NMR Biomed. 21:589 (2008); 3. Wheeler-Kingshott & Cercignani. MRM 61:1255 (2009); 4. Wheeler-Kingshott et al. Proc. of the XVII meeting of the ISMRM, p.3590 (2009); 5. Alexander et al., IEEE Trans Med Imaging 20:1131 (2001); 6. Salmond et al., Neuroimage 17:1027 (2002).

Acknowledgements: The Multiple Sclerosis Society of Great Britain and Northern Ireland and The Wellcome Trust for funding.